Published in final edited form as:
Magn Reson Imaging Clin N Am. 2010 February ; 18(1): 11–28. doi:10.1016/j.mric.2009.09.002.

MR Imaging–Guided Interventions in the Genitourinary Tract: An Evolving Concept

Fiona M. Fennessy, MD, PhD*, **Kemal Tuncali, MD**, **Paul R. Morrison, MSc**, and **Clare M. Tempany, MD**
Department of Radiology, Harvard Medical School/Brigham and Women's Hospital, 75 Francis Street, Boston, MA 02115, USA

Keywords

Uterine fibroids; Magnetic resonance guided focused ultrasound surgery (MRgFUS); Genitourinary tract; Prostate cancer; Radiofrequency ablation; Brachytherapy

MR imaging–guided interventions are a well-established form of routine patient care in many centers around the world. There are many different approaches, dependingonmagnetdesign and clinical need. The rationale behind this is based initially on MR imaging providing excellent inherent tissue contrast, without ionizing radiation risk for patients. MR imaging–guided minimally invasive therapeutic procedures have major advantages over conventional surgical procedures. In the genitourinary tract, MR imaging guidance can play a role in tumor detection, localization, and staging and can provide accurate image guidance for minimally invasive procedures for the confirmation of pathology, tumor treatment, and treatment monitoring. Depending on the body part accessed, a customizable magnet bore configuration and magnetic resonance (MR)-compatible devices can be made available. The advent of molecular and metabolic imaging and the use of higher strength magnets likely will improve diagnostic accuracy and allow patient-specific targeted therapy, designed to maximize disease control and minimize side effects.

GENITAL TRACT: FEMALE

One of the most unique and exciting MR-guided in-terventional procedures in the female pelvis is MR-guided focused ultrasound surgery (MRgFUS). In addition, MR is used to guide other interventions and therapies, such as biopsies and gynecologic tumor treatments. The latter have been done in several centers, guiding the placement of radiation catheters for delivery of high-dose radiation in cervical or endometrial cancer.[1]

*Corresponding author. ffennessy@partners.org (F.M. Fennessy).

MAGNETIC RESONANCE–GUIDED FOCUSED ULTRASOUND SURGERY FOR TREATING UTERINE FIBROIDS

Uterine fibroids are the most common female pelvic tumor, occurring in approximately 25% of women.[2] Although many patients remain asymptomatic, others suffer from symptoms, such as pelvic pain, menorrhagia, dysmenorrhagia, dyspareunia, urinary frequency, and infertility. Ultrasound (US) usually is the first diagnostic imaging modality of choice for fibroids, demonstrating a well-defined, usually hypoechoic mass. Providing good inherent tissue contrast, MR imaging is the optimal modality for fibroid detection, accurate localization, and volumetrics.

A wide spectrum of treatment options for uterine fibroids exists, ranging from expectant waiting to medical management to myomectomy to hysterectomy. Women, however, increasingly are seeking less invasive treatment options, perhaps motivated by fertility preservation and the possibility of reduced postprocedure recovery time. A good example of a less invasive choice is uterine artery embolization, a procedure that has demonstrated significant growth and interest since its introduction in 1995.[3] Only MRgFUS, however, is completely noninvasive. Approved by the United States Food and Drug Administration (FDA) in October 2004, much of the worldwide experience with MRgFUS has been with treatment of uterine fibroids, with more than 3500 patients treated to date.

Fundamentals of Magnetic Resonance–Guided Focused Ultrasound Surgery

The potential surgical application of focused ultrasound surgery (FUS) was first demonstrated in 1942.[4] Since then, it has been evaluated extensively in animal[5,6] and human[7] brains and in the kidney, prostate, liver, bladder,[8–11] and eye[12] within clinical trials. Clinical acceptance, however, was hampered because of the difficulty in controlling the focal spot position, defining the beam target precisely, and coping with the lack of feedback about thermal damage.

MR imaging can satisfy the requirements of FUS, having excellent anatomic resolution and high sensitivity for tumor visualization, thereby offering accurate planning of the tissue to be targeted. By exploiting the temperature dependence of the water proton resonant frequency,[13] MR-based temperature mapping is possible. This allows for targeting of the beam during subthreshold US exposures[14] and online estimation of the ablated volume.[15,16] Phase imaging is used to estimate the temperature-dependent proton resonant-frequency shift using a fast spoiled gradient-re-called-echo sequence (SPGR).[17] Therefore, obtaining temperature-sensitive MR images before, during, and after each sonication can monitor tissue temperature elevations, including any slight elevations in normal adjacent surrounding tissue, thereby preventing damage.

Magnetic Resonance–Guided Focused Ultrasound Surgery Equipment for Fibroid Treatment

Sonications are performed using an MR-compatible focused US system that is built into a table that docks with a compatible MR scanner. The system consists of a focused piezoelectric phasedarray transducer (208 elements, frequency 0.96–1.14 MHz) that is

located within the specially designed table surrounded by a water tank. A thin plastic membrane covers the water tank and allows the US beam to propagate into the tissue. Patients lie in a prone position in the magnet, with the anterior abdominal wall positioned over the water tank. The location of the focal spot is controlled electronically by the transducer array that controls the volume of coagulation necrosis.

Patient Selection for Magnetic Resonance–Guided Focused Ultrasound Surgery of Uterine Fibroids

The FDA has approved this procedure for premen-opausal women who have symptomatic uterine fibroids and who have no desire for future pregnancy. This treatment is not indicated for pregnant women, postmenopausal women, or those who have contraindications to contrast-enhanced MR imaging. If multiple fibroids are present, clinical symptomatology and accessibility to the target fibroids are reviewed and a target fibroid is selected. The anterior abdominal wall is evaluated for extensive scarring. Those women who have such scarring are excluded from treatment because of the risk for skin burns.[18]

Treatment Planning

Immediately before treatment, T2-weighted fast spin-echo images in three orthogonal planes are obtained to plan the beam path to the targeted lesion. The MR images are analyzed to evaluate the area to be treated for possible obstructions. Although patients who have extensive anterior abdominal wall scarring in the beam path generally are excluded at screening, it may be possible, however, to treat women who have abdominal wall scarring that is not extensive by angling the beam path, ensuring that the scar is not traversed (Fig. 1). Filling of the urinary bladder by Foley catheter clamping also may help in moving the uterus and selected fibroid into a position away from the abdominal wall scar. Coursing bowel loops lying anterior to the uterus at the level of the uterine fibroid also may cause treatment-planning difficulties. Placement of a gel spacing device may allow the bowel loops to be displaced out of the treatment field, thereby enlarging the acoustic window and allowing for greater treatment volume (Fig. 2).

Clinical Trials in the Treatment of Uterine Fibroids with Magnetic Resonance–Guided Focused Ultrasound Surgery

Multicenter clinical trials investigating the use of MRgFUS in the treatment of uterine fibroids, which subsequently resulted in device labeling by the FDA, were performed at five medical centers across the United States in addition to centers in the United Kingdom, Germany, and Israel. Follow-up of many patients is ongoing.

Enrollment for phase I/II began in 1999 to assess the safety and feasibility of MRgFUS in the treatment of fibroids. Eligible patients underwent MRgFUS followed by hysterectomy, and subsequent pathologic examination of the uterus and fibroid showed that MRgFUS did result in hemor-rhagic necrosis in the area of nonperfusion on the post-treatment MR.[19,20]

Phase III of the clinical trial involved treatment of larger volumes of fibroids in women who had symptomatic uterine fibroids who otherwise would have opted for hysterectomy (Fig. 3). To date, the longest-term follow-up—in 359 patients—is up to 24 months.[21] These

patients reported durable symptom relief. Those who had a greater nonperfused treatment volume fared better, with fewer of these patients undergoing additional fibroid treatment. These findings concur with those of Fennessy and colleagues,[22] where greater clinical outcome was found in those treated with a modified treatment protocol that allowed for greater nonperfused fibroid volumes post treatment.

CRYOTHERAPY FOR UTERINE FIBROIDS

MR-guided cryotherapy is a minimally invasive procedure. It involves a percutaneous approach in an interventional setting with multiple (1 to 5) needle-like 17-G cryotherapy probes. Each probe creates a tear-drop shaped volume of frozen tissue about its tip (approximately 2.5-mm diameter); the simultaneous use of multiple probes gives a larger volume of treated tissue in the same time frame as treating with a single probe. The freeze is provided by pressurized argon gas that circulates within the probe. Typical treatments involve a cycling of the gas that delivers a freeze-thaw-freeze to destroy tissue, with each stage of the cycle 10 to 15 minutes in duration. MR imaging–guided cryotherapy has been evolving through experiment and clinical use during the past 20 years to target a range of tumors in various organ systems.[23] Compared with US that has shadow artifacts, visibility of the ice ball for monitoring is not as limited.

There are several promising reports of MR imaging–guided cryotherapy to treat symptomatic patients who have uterine fibroids.[24–27] During cryotherapy, the ice appeared as a signal void in the image as a result of the short MR relaxation time of the solid ice, giving a clear demarcation between frozen and unfrozen tissue. Though all reported relief from deletorious symptoms, short-term clinical outcome, however, is reported in only 8 of 9 treated patients, who demonstrated on average, 65% volume reduction in uterine size.[25]

One of these studies[26] was performed transvaginally, with the investigators proposing that such an approach had the advantage of providing direct access, especially for submucosal tumors. Procedures usually are performed with epidural anesthesia in a horizontally open MR imaging scanner with multiple 2- to 3-mm cryotherapy probes (Fig. 4). Gradient-echo and T2-weighted spin-echo sequences were used to guide probe placement and monitor the treatment cycle of freeze-thaw-freeze (Fig. 5).

Percutaneous ablation of fibroids is a nascent procedure and not practiced widely. This method of ablation has found a place in treating other parts of the body but not necessarily treating uterine fibroids, possibly because of the recent emergence of other minimally invasive procedures, such as uterine artery embolization, or noninvasive procedures, such as MRgFUS.

GENITAL TRACT: MALE

The leading cause of cancer death in men over 50, prostate cancer, affects one man in six in his lifetime. The American Cancer Society estimates that in 2007 in the United States, 218,890 new cases of prostate cancer will be diagnosed, and approximately 27,050 men will die of the disease.[28] There is only a 33% 5-year survival rate in men who have metastatic disease,[29] making early tumor detection and localized treatment a necessity.

MR IMAGING–GUIDED PROSTATE BIOPSY

Early diagnosis and cancer localization within the prostate gland usually are found through digital examination and serum prostate-specific antigen (PSA) measurement, followed by transrectal ultrasound (TRUS)-guided biopsy. Image-guided prostate biopsy with ultrasound (US) has become a universally accepted tool,[30] but because of a low sensitivity and specificity for tumor detection,[31] interest continues in the development of a more accurate technique. In addition, for men who have increasing PSA levels and repeatedly negative TRUS-guided prostate biopsies (the concern being that a sampling error may result in a false-negative biopsy), for those in whom a transrectal biopsy is not possible, or for those who are reluctant to undergo transrectal biopsy because of its recognized complications, such as infection, hematuria, hematospermia, and rectal bleeding,[32–34] an alternative approach may be necessary.

MR imaging can outline prostate architecture and substructure. Although the specificity for diagnosis may be limited, MR imaging can demonstrate suspicious nodules in the peripheral zone, the most common site for prostate cancer. On T2-weighted images, tumor is demonstrated most commonly by focal or diffuse regions of decreased signal intensity relative to the high-signal-intensity normal peripheral zone. MR imaging is used most routinely for staging men who have known cancer. The reported accuracy of prostate cancer detection and staging on MR images varies widely, with reports of accuracy ranging from 54% to 93%, likely because of differences in techniques and interobserver variability.[35–38]

Its role in detection and characterization, particularly in the initial diagnosis of high-risk patients or those who have previous negative biopsy findings but persistently high PSA levels, is increasing as techniques such as MR spectroscopy imaging (MRSI) and dynamic contrast enhancement become more widely available. The ultimate role and application in clinical practice, however, remain controversial.[35] MR imaging contributes significant incremental value to TRUS-guided biopsy and digital rectal examination in cancer detection and localization in the prostate.[39] It offers an excellent second-line alternative to those who have failed to obtain a diagnosis with conventional methods.

MR Imaging–Guided Prostate Biopsy: Technique

Two basic strategies have been explored for MR imaging–guided prostate biopsy. The first is coregistration of previously acquired diagnostic MR images to TRUS images, localizing suspected tumor lesions on MR and correlating these locations to the US.[40] The second strategy is stereotactic needle interventions within diagnostic MR scanners using careful patient positioning. By implementing surgical navigation software originally developed for neurosurgery[41,42] and adapting the technical capabilities of MR imaging–guided prostate brachytherapy in an open configuration magnet,[43] biopsy of suspected tumor foci in the peripheral zone is made possible (Fig. 6).[44] In addition, the feasibility of transrectal needle access to prostate tumors has been assessed in a closed-bore 1.5-T magnet[45–48] in a small number of patients, which potentially could provide for additional functional and spectroscopic imaging in comparison with a 0.5-T scanner. The procedure requires the use of a specialized device that consists of a needle guide and support system. The same guidance also has been used recently in a 3-T system.[49] Larger studies of clinical usefulness,

however, are necessary. With progress in biologic imaging of the prostate gland, it is likely that MR imaging guidance will play an increasing role in the diagnosis and treatment of prostate cancer.

MR Imaging–Guided Prostate Biopsy: The Future

The move toward targeted interventions, for diagnosis and treatment, underscores the need for precise image-guided needle placement. Based on a patient's anatomy and lesion detection in pretreatment MR imaging, a graphic planning interface that allows desired needle trajectories to be specified, through MR-compatible robotic assistance, recently has been described.[50] Avoiding the limitations of a fixed-needle template is a positive move forward for tissue sampling and treatment. As the field of prostate imaging moves to higher strength magnets, namely 3 T, the biopsy devices are reconfigured to allow sampling in a closed-bore environment. A recent studyof prostate biopsy using 3-T MR imaging guidance described it as a promising tool for detecting and sampling cancerous regions in patients who have known prostate cancer[49]; however, the role (even at 3 T) of MR imaging–guided prostate biopsy as a screening tool in patients who have elevated PSA levels and recent previous negative biopsy remains to be determined.

MR IMAGING–GUIDED BRACHYTHERAPY FOR PROSTATE CANCER

Established options for the management of localized prostate cancer include one or a combination of the following: radical prostatectomy, external beam radiation therapy, brachytherapy, or watchful waiting. In radiation therapy, the goal is to achieve the prescribed dose throughout the prostate gland while minimizing toxicity to adjacent structures and minimizing morbidity from the procedure. Prostate brachytherapy is one of the more popular radiation methods in the prostate and involves the percutaneous placement of I-125 radiation seeds into the gland under image guidance. This is done most commonly with TRUS. It also can be done with MR guidance and the goal in both procedures is to optimize seed placement and allow maximal dose to the prostate peripheral zone tumor and minimal dose to the urethra and rectum.

Imaging-guided radiation therapy, therefore, allows directed tumor treatment, decreasing the chances of disease spreading outside the gland, while healthy prostate tissue and its neighboring structures are not overdosed. This is extremely important for structures such as the urethra, in which over-radiation may cause stricture and fistu-alization that can be avoided with good image guidance.[51,52] Radiation dose fall-off is sharp at the rectal wall and at the urethra. Unlike external beam radiotherapy, there is no entrance or exit dose. Brachytherapy, therefore, has the potential to achieve superior tumor control with decreased morbidity and side effects. It is not, however, without its own set of complications, such as rectal irritation and ulceration, incontinence, and impotence resulting from inadvertent delivery of radiation dosing to the rectum, bladder, and urethra.

Patient Selection

Low-risk prostate cancer patients who have a high probability of organ-confined disease are screened appropriately with an endorectal coil MR for potential treatment with

brachytherapy monotherapy. Most centers include patients who have stage T1-T2a (according to the American Joint Committee on Cancer/International Union Against Cancer 1997 staging), PSA level of 10 ng/mL or less, and a Gleason score of 6 or lower. The few contraindications to the procedure include prior transurethral resection of the prostate or morbid obesity (equipment cannot sustain the weight).

Procedure

MR-guided prostate brachytherapy using open configuration 0.5-T and 1.5-T scanners are described.[43,45] Using the open 0.5-T magnet, patients are placed supine between the two magnets in the lithotomy position under general anesthesia. A Foley catheter is inserted, the skin is prepared and draped in a sterile fashion, and a template for needle guidance is placed against the perineum. A rectal obturator then is placed and T2-weighted images are acquired in the axial, coronal, and sagittal planes and used to outline the urethra, peripheral zone, and anterior rectal wall. Surgical simulation software outlines these areas, and the targeted volume is calculated using designated planning software.[53] Seed number and depth of catheter insertion are calculated.

While gradient-echo MR images are obtained in real time,[44] seed-loaded catheters then are positioned in the prostate gland (Fig. 7). The images are compared to their intended locations, according to the radiation therapist plan. Dose-volume histograms of the urethra, anterior rectal wall, and target volume are obtained before final deployment of seeds. Six weeks after the procedure, CT imaging (to identify the seeds accurately) and MR imaging (for prostate anatomic correlation) are fused to calculate the final dose distribution to the gland and surrounding tissues.

Although open-bore magnets offer good patient accessibility and allow satisfactory prostate tumor and anatomic depiction, higher-quality MR intervention images in a closed 1.5-T system also have been investigated.[45] This system uses a customized perineal template, an endorectal imaging coil, and a lockable positioning arm. Patients are placedinthe leftlateral decubitus position. Although patient accessibility with this technique may be limited because of the closed-bore configuration and the 60-cm diameter bore, the investigators found that dependence on deformable registration between image sets (high-field 1.5-T diagnostic images and low-field–strength interventional images) was reduced.

Outcomes

Short-term toxicity after MR-guided brachytherapy is rare, with no gastrointestinal or sexual dysfunction reported during the first month after treatment.[54] Within 24 hours of removal of the Foley catheter, acute urinary retention was reported in 12% of men, which was self-limited to within 1 to 3 weeks of treatment. Prostatic volume and transitional zone volume, determined by MR imaging, and number of brachy therapy seeds placed were found to be significant predictors of acute urinary retention.

The long-term genitourinary and rectal toxicity was compared between those who received MR-guided brachytherapy alone and those who received combined MR-guided brachytherapy and external beam radiation therapy.[55] The 4-year estimates of rectal bleeding requiring coagulation for patients who underwent MR-guided brachy-therapy

compared with patients who received combined-modality therapy were 8% versus 30%. The 4-year estimate of freedom from radiation cystitis was 100% versus 95% for patients who received MR-guided brachytherapy alone and patients who received combined-modality therapy, respectively. In a separate study evaluating the long-term toxicity in patients who received MR-guided brachytherapy as a salvage procedure for radiation therapy failure,[56] the 4-year estimate of grade 3 or 4 gastrointestinal or genitourinary toxicity was reported at 30% of all patients, with 13% requiring an intervention, such as a colostomy or urostomy for fistula repair.

Supplemental external beam radiotherapy, in addition to brachytherapy seed implantation, has been given to patients who have intermediate- to high-risk prostate cancer (according to the D'Amico risk stratification for prostate cancer).[57] This combination of radiation therapy has demonstrated good long-term results,[58,59] resulting in a 15-year biochemical relapse-free survival equal to 80.3% for intermediate-risk disease and 67.2% for high-risk disease.

Brachytherapy: The Future

The current manual method of needle placement, using a fixed-needle template guide, constrains needle orientation. The manual method also makes use of manual computation and transcription of needle coordinates that are prone to human error. The future points toward a system that incorporates an interactive planning interface with MR-compatible robotic assistance. Such a device, which serves as a dynamic guide for precise needle placement, has been developed.[60] Likely the future direction for percutaneous MR imaging–guided prostatic interventions, this MR-compatible robotic device has been integrated with a software planning interface, allowing physicians to specify desired needle trajectories based on MR imaging anatomy.

FOCUSED ULTRASOUND SURGERY IN THE PROSTATE

As discussed previously regarding the female genital tract, there is growing interest in MRgFUS because of its many potential applications as a minimally invasive therapy. US-guided FUS (USgFUS) has been used predominantly in Europe for the treatment of prostate cancer. Limitations include difficulty in treating the anterior prostate or small-volume prostates, and lack of long-term follow-up.

Literature describing the results of USgFUS for prostate cancer suggests that USgFUS treatment is a valuable option for well-differentiated and moderately differentiated tumors and for local recurrence after external-beam radiation therapy.[61–63] USgFUS treatment is whole-gland therapy, without selective tumor-directed targeted treatment, that should allow for minimal disruption of normal function. USgFUS arguably is limited by the lack of direct temperature and thermal dose measurements during thermocoagulation. Without the latter, the energy delivery cannot be controlled or monitored nor can the thermal dose be measured accurately.

To address these challenges, MR imaging–compatible prostate applications have been developed for hyperthermia,[64] and phased-array applicators for thermal ablation.[65] Insightec (Haifa, Israel) has developed a MRgFUS system for prostate treatment (Fig. 8). A major

potential advantage of MR imaging guidance is its ability to map functional changes in prostate tissue, with the possibility of 3-D tumor mapping before and during treatment. Overall, noninvasive thermal ablation using MR imaging guidance should improve prostate treatment significantly and its application should increase in the near future.

MR IMAGING–GUIDED CATHETER-BASED ULTRASOUND THERMAL THERAPY OF THE PROSTATE

In a similar mode, catheter-based US devices (in interstitial and transurethral configurations) have been evaluated in canine prostate models in vivo and found to produce spatially selective regions of thermal destruction in the prostate.[66–68] Transurethral US devices with tubular transducers have been developed, which can coagulate sectors of the prostate using pre-shaped angular patterns.[69,70] Devices with finer spatial control using planar[71,72] or curvilinear transducers[73] can be rotated slowly using a computer-controlled, MR-compatible stepper motor while under MR imaging guidance and feedback (Fig. 9). The feasibility of MR imaging–guided interstitial US thermal therapy of the prostate has been evaluated in an in vivo canine prostate model.[66] MR imaging–compatible, multielement interstitial US applicators were used. The applicators were inserted transperineally into the prostate with the energy directed ventrally away from the rectum. This study demonstrated a large volume of ablated tissue within the prostate and, importantly, demonstrated contiguous zones of thermal coagulation. At least in an animal model and using MR guidance, transurethral and interstitial treatment strategies have, therefore, demonstrated significant potential for thermal ablation of localized prostate cancer.

URINARY TRACT

Renal cell carcinoma (RCC) is the sixth leading cause of cancer death,[74] and its incidence in the United States is rising.[75] Partial nephrectomy, a nephron-sparing surgical method, has replaced radical nephrectomy for the treatment of small RCC. Less invasive methods also have emerged that can be performed laparoscopically (partial nephrectomy and cryosurgery) or percutaneously (radiofrequency ablation [RFA] and cryoablation). Image-guided percutaneous ablations have the potential to replace others as the least invasive and least costly[76] of all nephron-sparing treatments clinically available, particularly in patients who are poor surgical candidates because of comorbid disease and patients who have renal insufficiency, solitary kidney, or multiple RCC.

MR IMAGING–GUIDED RADIOFREQUENCY ABLATION IN THE KIDNEY

RFA is a focal thermal tumor therapy method in which tissue is heated by an electric current. The current is present with a high density surrounding a percutaneously placed electrode that is driven by an electrical generator. The circuit is completed by the placement of grounding pads on a patient. The electrode is placed interstitially and intended to be activated to create a volume of coagulative necrosis in place of the tumor.

Many reports of successful treatment of renal tumors with percutaneous RFA have been published.[77–85] Real-time monitoring of RFA, however, is not possible with CT or US

because the thermal ablation zone is not visible with these imaging modalities. RFA can be monitored with MR imaging.[86,87]

But with limitations. Radiofrequency energy has to be interrupted during MR imaging because of the significant interference it causes otherwise. Furthermore, the temperature-sensitive, very short repetition time/echo time gradient-echo sequences typically are not suitable for detailed visualization of retroperitoneal anatomy.

Specific to MR imaging-guided RFA in the kidney , the first report was an in vivo study in porcine kidney.[88] The procedures were performed in a 0.2-T open magnet and demonstrated the suitability of MR imaging for guiding needle placement and the benefit of its inherent soft-tissue sensitivity where the electrode could be placed and the thermal lesion observed. Clinical studies of MR imaging–guided RFA in the kidney subsequently reported the safety and efficacy of the procedure[87,89] in tumors less than4cmindiameter.Norecurrencesat25months' post procedure were reported.

Overall, RFA is a feasible therapeutic modality for kidney lesions, under MR imaging, CT, or US guidance.[90] Although RFA is performed more routinely under CT guidance, many practices turn to MR imaging for the assessment and long-term follow-up of treated patients.[91–93]

MR IMAGING–GUIDED PERCUTANEOUS CRYOTHERAPY OF RENAL TUMORS

Cryoablation, a focal thermal tumor therapy method which uses extreme cold to establish coagulative necrosis, has several advantages over RFA. While RFA may require the need to perform multiple overlapping ablations of larger tumors, with percutaneous cryoablation, larger tumors can be treated simultaneously with the placement of multiple applicators.[94,95] Evidence suggests that renal tumors more likely are treated in one session with cryoablation compared to RFA.[96] Lower doses of medications are required for intravenous conscious sedation suggesting that percutaneous cryoablation of renal tumors is associated with less intraprocedural pain than with percutaneous RFA.[97]

US monitoring of cryoablation is limited by an inability to image the entire ice ball because of acoustic shadowing from the edge closest to the US probe.[98] Cryoablation of renal tumors can be monitored with CT because the ice ball is readily apparent as a hypoattenuating structure in the renal parenchyma.[94,95,98–103] There are two main limitations with CT, however. One is that the portion of the ice ball in the perinephric fat, a hyper-attenuating region, provides only a modest contrast-to-noise ratio[104,105] compared to surrounding fat, and the ablation zone edge is not demarcated clearly in fatty tissue (Fig. 10A). This limits its use for real-time monitoring of the effect of ablation on adjacent critical structures, such as bowel, ureter, pancreas, and adrenal gland. Another is that the streak artifact created by the applicators with CT imaging can interfere with ice ball visibility (Fig. 10B).

Since the initial clinical reports of MR imaging–guided percutaneous cryoablation of renal tumors[98,100] in 2001, several investigators have shown the feasibility and safety of the

procedure,[106–112] all demonstrating the advantages of MR imaging monitoring during percutaneous cryoablation procedures.

MR imaging depicts the ice ball as a signal void region with high contrast-to-noise ratio compared to surrounding tissues, with sharp edge definition in multiple planes and with minimal applicator artifact (Fig. 11). Ice ball volume on intraprocedural MR imaging correlates well with volume of cryo-necrosis on postprocedural MR imaging.[113] Because the ice ball is well depicted on all pulse sequences, the ablation can be monitored using pulse sequences that display tumor or adjacent critical structures best.[111] If images demonstrate incomplete coverage of tumor, additional applicators may be placed to improve coverage.[111,112] Alternatively, if the ice ball edge approaches adjacent critical structures, the freezing can be stopped.[111] Applicators can be controlled individually. Additional maneuvers to reduce risk for injury to surrounding bowel, such as water instillation described for CT-guided ablations,[114] also can be performed during MR imaging–guided cryoablations.[111] A noninvasive method of external manual displacement of bowel during MR imaging–guided cryoablation of renal tumors also is described—a maneuver unique to cryoablation procedures performed in an open-configuration interventional MR imaging unit.[115]

Limitations of MR imaging–guided cryoablation include the high cost of MR imaging units and its limited availability, generally long procedure times, smaller gantry sizes compared to CT scanners, and inability to detect ST-T segment changes of cardiac ischemia on an EKG in the magnetic environment during procedures.

In summary, image-guided percutaneous ablative therapies have the potential to replace conventional surgical treatment of small RCC. Compared with other image-guided ablative therapies, with its vast advantages and minimal limitations, MR imaging–guided percutaneous cryoablation is well poised to play an important role in the management of renal tumors.

THE FUTURE

Recent developments in MR imaging paralleling those in computer-assisted surgery have set up an ideal environment for MR-compatible robotic systems and manipulators. Materials used in mechatronic devices inside the magnet ideally should have a magnetic susceptibility similar to that of human tissue and be electrical insulators to avoid image distortion. Although image quality is reduced because of reduction in static field strength, interventional open-bore magnets have fewer spatial constraints. Alternatively, closed MR scanners can impose severe constraints on procedural manipulations, despite their imaging advantage of higher field strengths. New wide-and short-bore 1.5-T magnets (Espree, Siemens, Erlangen, Germany) will expand the use of interventional MR imaging. Emerging use of 3-T magnets for interventions will bring about improved monitoring of thermal therapies. Much research is underway evaluating material selection, position detection sensors, different actuation models and techniques, and design strategies.[116] Once the engineering hurdle is overcome, systems must undergo clinical validation before introduction into the commercial realm.

SUMMARY

MR imaging has become part of routine care in many places around the world, for tumor detection, localization, and staging. In the genitourinary tract, MR imaging guidance is playing an increasing role in minimally invasive procedures for confirmation of tumor pathology and for tumor treatment and treatment monitoring. It offers inherent ability for tumor detection and biopsy guidance and, currently, MR-guided ablative therapies are an increasing and real alternative to more invasive surgical options. As the capabilities of MR imaging expand and newer imaging modalities become more accessible (PET imaging, for example), the need for nonrigid registration of multiple modalities will be necessary. A combination of functional imaging and high-resolution tumor detail in the genitourinary tract, in a patient-specific treatment environment, should increase demand and the use of semi-invasive or noninvasive technology. Clearly, the pressure is on to provide MR-compatible devices and methodology that easily integrate with imaging and are supportive of patients' clinical needs.

Acknowledgments

This work was supported in part by National Institutes of Health grant U41RR019703.

References

1. Stewart AJ, Viswanathan AN. Current controversies in high-dose-rate versus low-dose-rate brachytherapy for cervical cancer. Cancer. 2006; 107(5):908–15. [PubMed: 16874815]
2. Stewart EA. Uterine fibroids. Lancet. 2001; 357:293–8. [PubMed: 11214143]
3. Ravina J, Herbreteau D, Ciraru-Vigneron N, et al. Arterial embolisation to treat uterine myomata. Lancet. 1995; 346:671–2. [PubMed: 7544859]
4. Lynn JG, Zwemer RL, Chick AJ, et al. A new method for the generation and use of focused ultrasound in experimental biology. J Gen Physiol. 1942; 26:179–93. [PubMed: 19873337]
5. Fry WJ, Barnard JW, Fry FJ. Ultrasonically produced localized selective lesions in the central nervous system. Am J Phys Med. 1955; 34:413–23. [PubMed: 14376518]
6. Lele PP. A simple method for production of trackless focal lesions with focused ultrasound: physical factors. J Physiol. 1962; 160:494–512. [PubMed: 14463953]
7. Heimburger RF. Ultrasound augmentation of central nervous system tumor therapy. Indiana Med. 1995; 78:469–76. [PubMed: 4020091]
8. Gelet A, Chapelon JY, Bouvier R, et al. Local control of prostate cancer by transrectal high intensity focused ultrasound therapy: preliminary results. J Urol. 1999; 161:156–62. [PubMed: 10037389]
9. Paterson RF, Barret E, Siqueira TM Jr, et al. Laparoscopic partial kidney ablation with high intensity focused ultrasound. J Urol. 2003; 169(1):347–51. [PubMed: 12478187]
10. Yang R, Sanghvi NT, Rescorla FJ, et al. Extracorporeal liver ablation using sonography-guided high-intensity focused ultrasound. Invest Radiol. 1992; 27(10):796–803. [PubMed: 1399435]
11. Watkin NA, Morris SB, Rivens IH, et al. A feasibility study for the non-invasive treatment of superficial bladder tumours with focused ultrasound. Br J Urol. 1996; 78(5):715–21. [PubMed: 8976766]
12. Lizzi FL, Deng CX, Lee P, et al. A comparison of ultrasonic beams for thermal treatment of ocular tumors. Eur J Ultrasound. 1999; 9(1):71–8. [PubMed: 10099168]
13. Ishihara Y, Calderon A, Watanabe H, et al. A precise and fast temperature mapping using water proton chemical shift. Magn Reson Med. 1995; 34(6):814–23. [PubMed: 8598808]
14. Hynynen K, Vykhodtseva NI, Chung AH, et al. Thermal effects of focused ultrasound on the brain: determination with MR imaging. Radiology. 1997; 204(1):247–53. [PubMed: 9205255]

15. Chung AH, Jolesz FA, Hynynen K. Thermal dosimetry of a focused ultrasound beam in vivo by magnetic resonance imaging. Med Phys. 1999; 26(9):2017–26. [PubMed: 10505893]
16. McDannold N, Tempany CM, Fennessy FM, et al. Uterine leiomyomas: MR imaging-based thermometry and thermal dosimetry during focused ultrasound thermal ablation. Radiology. 2006; 240(1):263–72. [PubMed: 16793983]
17. Chung AH, Hynynen K, Colucci V, et al. Optimization of spoiled gradient-echo phase imaging for in vivo localization of focused ultrasound beam. Magn Reson Med. 1996; 36(5):745–52. [PubMed: 8916025]
18. Leon-Villapalos J, Kaniorou-Larai M, Dziewulski P. Full thickness abdominal burn following magnetic resonance guided focused ultrasound therapy. Burns. 2005; 31(8):1054–5. [PubMed: 15970389]
19. Tempany CM, Stewart EA, McDannold N, et al. MR imaging-guided focused ultrasound surgery of uterine leiomyomas: a feasibility study. Radiology. 2003; 226(3):897–905. [PubMed: 12616023]
20. Stewart EA, Gedroyc WM, Tempany CM, et al. Focused ultrasound treatment of uterine fibroid tumors: safety and feasibility of a noninvasive thermoablative technique. Am J Obstet Gynecol. 2003; 189(1):48–54. [PubMed: 12861137]
21. Stewart EA, Gostout B, Rabinovici J, et al. Sustained relief of leiomyoma symptoms by using focused ultrasound surgery. Obstet Gynecol. 2007; 110(2 Pt 1):279–87. [PubMed: 17666601]
22. Fennessy FM, Tempany C, McDannold N, et al. Uterine leiomyomas: MR imaging-guided focused ultrasound surgery–results of different treatment protocols. Radiology. 2007; 243(3):885–93. [PubMed: 17446521]
23. Morrison PR, Silverman SG, Tuncali K, et al. MRI guided cryotherapy. J Magn Reson Imaging. 2008; 27(2):410–20. [PubMed: 18219676]
24. Sewell PE, Arriola RM, Robinette L, et al. Real-time I-MR-imaging-guided cryoablation of uterine fibroids. J Vasc Interv Radiol. 2001; 12(7):891–3. [PubMed: 11435548]
25. Cowan BD, Sewell PE, Howard JC, et al. Interventional magnetic resonance imaging cryotherapy of uterine fibroid tumors: preliminary observation. Am J Obstet Gynecol. 2002; 186(6):1183–7. [PubMed: 12066095]
26. Dohi M, Harada J, Mogami T, et al. MR-guided transvaginal cryotherapy of uterine fibroids with a horizontal open MRI system: initial experience. Radiat Med. 2004; 22(6):391–7. [PubMed: 15648454]
27. Sakuhara Y, Shimizu T, Kodama Y, et al. Magnetic resonance-guided percutaneous cryoablation of uterine fibroids: early clinical experiences. Cardiovasc Intervent Radiol. 2006; 29(4):552–8. [PubMed: 16532267]
28. American Cancer Society. Cancer facts and figures 2007. Atlanta (GA): American Cancer Society; 2006. Publication no. 500807
29. American Cancer Society. Cancer facts and figures. Atlanta (GA): American Cancer Society; 2008. Publication no. 500807
30. Lee F, Gray JM, McLeary RD, et al. Prostatic evaluation by transrectal sonography: criteria for diagnosis of early carcinoma. Radiology. 1986; 158:91–5. [PubMed: 3510031]
31. Terris MK. Sensitivity and specificity of sextant biopsies in the detection of prostate cancer; preliminary report. Urology. 1999; 54:486–9. [PubMed: 10475359]
32. Aus G, Hermansson CG, Hugosson J, et al. Transrectal ultrasound examination of the prostate: complications and acceptance by patients. Br J Urol. 1993; 71:457–9. [PubMed: 8499990]
33. Collins GN, Lloyd SN, Hehir M, et al. Multiple transrectal ultrasound-guided prostatic biopsies: true morbidity and patient acceptance. Br J Urol. 1993; 71:460–3. [PubMed: 8499991]
34. Rodriguez LV, Terris MK. Risks and complications of transrectal ultrasound guided prostate needle biopsy: a prospective review of the literature. J Urol. 1998; 160:2115–20. [PubMed: 9817335]
35. Rifkin MD, Zerhouni EA, Gatsonis CA, et al. Comparison of magnetic resonance imaging and ultrasonography in staging early prostate cancer: results of a multi-institutional cooperative trial. N Engl J Med. 1990; 323:621–6. [PubMed: 2200965]

36. Schnall MD, Pollack HM. Magnetic resonance imaging of the prostate gland. Urol Radiol. 1990; 12(2):109–14. [PubMed: 1700526]
37. Cornud F, Flam T, Chauveinc L, et al. Extraprostatic spread of clinically localized prostate cancer: factors predictive of pT3 tumor and of positive endorectal MR imaging examination results. Radiology. 2002; 224(1):203–10. [PubMed: 12091684]
38. Outwater EK, Petersen RO, Siegelman ES, et al. Prostate carcinoma: assessment of diagnostic criteria for capsular penetration on endorectal coil MR images. Radiology. 1994; 193(2):333–9. [PubMed: 7972739]
39. Mullerad M, Hricak H, Kuroiwa K, et al. Comparison of endorectal magnetic resonance imaging, guided prostate biopsy and digital rectal examination in the preoperative anatomical localization of prostate cancer. J Urol. 2005; 174:2158–63. [PubMed: 16280755]
40. Perrotti M, Han KR, Epstein RE, et al. Prospective evaluation of endorectal magnetic resonance imaging to detect tumor foci in men with prior negative prostatic biopsy: a pilot study. J Urol. 1999; 162:1314–7. [PubMed: 10492187]
41. Hata N, Morrison PR, Kettenbach J, et al. Computer-assisted intra-operative MRI monitoring of interstitial laser therapy in the brain: a case report. SPIE J Biomed Optics. 1998; 3:302–11.
42. Gering, D.; Nabavi, A.; Kikinis, R., et al. An integrated visualization system for surgical planning and guidance using image fusion and interventional imaging; Medical Image Computing and Computer-Assisted Intervention (MICCAI); Cambridge, England. September 22, 1999;
43. D'Amico AV, Cormack R, Tempany CM, et al. Realtime magnetic resonance image-guided interstitial brachytherapy in the treatment of select patients with clinically localized prostate cancer. Int J Radiat Oncol Biol Phys. 1998; 42:507–15. [PubMed: 9806508]
44. Hata N, Jinzaki M, Kacher D, et al. MR imaging-guided prostate biopsy with surgical navigation software; device validation and feasibility. Radiology. 2001; 220:263–8. [PubMed: 11426008]
45. Susil RC, Camphausen K, Choyke P, et al. System for prostate brachytherapy and biopsy in a standard 1. 5 T MRI scanner Magn Reson Med. 2004; 52(3):683–7.
46. Susil RC, Menard C, Kreiger A, et al. Transrectal prostate biopsy and fiducial marker placement in a standard 1.5T magnetic resonance imaging scanner. J Urol. 2006; 175(1):113–20. [PubMed: 16406885]
47. Beyersdorff D, Winkel A, Hamm B, et al. MR imaging-guided prostate biopsy with a closed MR unit at 1.5 T: initial results. Radiology. 2005; 234(2):576–81. [PubMed: 15616117]
48. Kreiger A, Susil RC, Menard C, et al. Design of a novel MRI compatible manipulator for image guided prostate interventions. IEEE Trans Biomed Eng. 2005; 52(2):306–13. [PubMed: 15709668]
49. Singh AK, Kreiger A, Lattouf JB. Patient selection determines the prostate cancer yield of dynamic contrast-enhanced magnetic resonance imaging-guided transrectal biopsies in a closed 3-Tesla scanner. BJU Int. 2008; 101(12):181–5. [PubMed: 17922874]
50. DiMaio SP, Pieper S, Chinzei K, et al. Robot-assisted needle placement in open MRI: system architecture, integration and validation. Comput Aided Surg. 2007; 12(1):15–24. [PubMed: 17364655]
51. Lee WR, Hall MC, McQuellon RP, et al. A prospective quality-of-life study in men with clinically localized prostate carcinoma treated with radical prostatectomy, external beam radiotherapy, or interstitial brachytherapy. Int J Radiat Oncol Biol Phys. 2001; 51(3):614–23. [PubMed: 11597800]
52. Zelefsky MJ, Yamada Y, Marion C, et al. Improved conformality and decreased toxicity with intraoperative computer-optimized transperineal ultrasound-guided prostate brachytherapy. Int J Radiat Oncol Biol Phys. 2003; 55(4):956–63. [PubMed: 12605973]
53. Kooy HM, Cormack RA, Mathiowitz RV, et al. A software system for interventional magnetic resonance image-guided prostate brachytherapy. Comput Aided Surg. 2000; 5(6):401–13. [PubMed: 11295853]
54. D'Amico AV, Cormack R, Kumar S, et al. Real-time magnetic resonance imaging-guided brachytherapy in the treatment of selected patients with clinically localized prostate cancer. J Endourol. 2000; 14:367–70. [PubMed: 10910153]
55. Albert M, Tempany CM, Schultz, et al. Late genitourinary and gastrointestinal toxicity after magnetic resonance image-guided prostate brachytherapy with or without neoadjuvant external beam radiation therapy. Cancer. 2003; 98(5):949–54. [PubMed: 12942561]

56. Nguyen PL, Chen MH, D'Amico AV, et al. Magnetic resonance image-guided salvage brachytherapy after radiation in select men who initially presented with favorable-risk prostate cancer: a prospective phase 2 study. Cancer. 2007; 110(7):1485–92. [PubMed: 17701957]
57. D'Amico AV, Moul J, Carroll PR, et al. Cancer-specific mortality after surgery or radiation for patients with clinically localized prostate cancer managed during the prostate-specific antigen era. J Clin Oncol. 2003; 21(11):2163–72. [PubMed: 12775742]
58. Sylvester JE, Grimm PD, Blasko JC, et al. 5-Year biochemical relapse free survival in clinical Stage T1–T3 prostate cancer following combined external beam radiotherapy and brachytherapy; Seattle experience. Int J Radiat Oncol Biol Phys. 2007; 67(1):57–64. [PubMed: 17084544]
59. Lawton CA, DeSilvo M, Lee WR, et al. Results of a phase II trial of transrectal ultrasound-guided permanent radioactive implantation of the prostate for definitive management of localized adenocarcinoma of the prostate (radiation therapy oncology group 98-05). Int J Radiat Oncol Biol Phys. 2007; 67(1):39–47. [PubMed: 17084551]
60. Chinzei K, Miller K. Towards MRI guided surgical manipulator. Med Sci Monit. 2001; 7:153–63. [PubMed: 11208513]
61. Poissonier L, Chapelon JY, Rouviere O, et al. Control of prostate cancer by transrectal HIFU in 227 patients. Eur Urol. 2007; 51(2):381–7. [PubMed: 16857310]
62. Uchida T, Ohkusa H, Nagata Y, et al. Treatment of localized prostate cancer using high-intensity focused ultrasound. BJU Int. 2006; 97(1):56–61. [PubMed: 16336329]
63. Ficarra V, Antoniolli SZ, Novara G, et al. Short-term outcome after high-intensity focused ultrasound in the treatment of patients with high-risk prostate cancer. BJU Int. 2006; 98(6):1193–8. [PubMed: 17125477]
64. Smith NB, Buchanan MT, Hynynen K. Transrectal ultrasound applicator for prostate heating monitored using MRI thermometry. Int J Radiat Oncol Biol Phys. 1999; 43(1):217–25. [PubMed: 9989529]
65. Sokka SD, Hynynen KH. The feasibility of MRI-guided whole prostate ablation with a linear aperiodic intracavitary ultrasound and phased array. Phys Med Biol. 2000; 45(11):3378–83.
66. Nau WH, Diederich CJ, Ross AB, et al. MRI-guided interstitial ultrasound thermal therapy of the prostate: a feasibility study in the canine model. Med Phys. 2005; 32(3):733–43. [PubMed: 15839345]
67. Pauly KB, Diedrich CJ, Rieke V, et al. Magnetic resonance-guided high-intensity ultrasound ablation of the prostate. Top Magn Reson Imaging. 2006; 17(3):195–207. [PubMed: 17414077]
68. Diederich CJ, Nau WH, Ross AB, et al. Catheter-based ultrasound applicators for selective thermal ablation: progress towards MRI-guided applications in prostate. Int J Hyperthermia. 2004; 20(7): 739–56. [PubMed: 15675669]
69. Diederich CJ, Stafford RJ, Nau WH, et al. Transurethral ultrasound applicators with directional heating patterns for prostate thermal therapy: in vivo evaluation using magnetic resonance thermometry. Med Phys. 2004; 31(2):405–13. [PubMed: 15000627]
70. Hazle JD, Diederich CJ, Kangasniemi M, et al. MRI-guided thermal therapy of transplanted tumors in the canine prostate using a directional transurethral ultrasound applicator. J Magn Reson Imaging. 2002; 15(4):409–17. [PubMed: 11948830]
71. Chopra R, Burtnyk M, Haider MA, et al. Method for MRI-guided conformal thermal therapy of prostate with planar transurethral ultrasound heating applicators. Phys Med Biol. 2005; 50(21): 4957–75. [PubMed: 16237234]
72. Ross AB, Diederich CJ, Nau WH, et al. Highly directional transurethral ultrasound applicators with rotational control for MRI guided prostatic thermal therapy. Phys Med Biol. 2004; 49(1): 189–204. [PubMed: 15083666]
73. Ross AB, Diederich CJ, Nau WH, et al. Curvilinear transurethral ultrasound applicator for selective prostate thermal therapy. Med Phys. 2005; 32(6):1555–65. [PubMed: 16013714]
74. Godley PA, Ataga KI. Renal cell carcinoma. Curr Opin Oncol. 2000; 12:260–4. [PubMed: 10841199]
75. Chow WH, Devesa SS, Warren JL, et al. Rising incidence of renal cell cancer in the United States. JAMA. 1999; 281:1628–31. [PubMed: 10235157]

76. Link RE, Permpongkosol S, Gupta A, et al. Cost analysis of open, laparoscopic, and percutaneous treatment options for nephron-sparing surgery. J Endourol. 2006; 20:782–9. [PubMed: 17094755]
77. Gervais DA, McGovern FJ, Wood BJ, et al. Radio-frequency ablation of renal cell carcinoma: early clinical experience. Radiology. 2000; 217:665–72. [PubMed: 11110926]
78. Ogan K, Jacomides L, Dolmatch BL, et al. Percutaneous radiofrequency ablation of renal tumors: technique, limitations, and morbidity. Urology. 2002; 60:954–8. [PubMed: 12475648]
79. Farrell MA, Charboneau WJ, DiMarco DS, et al. Imaging-guided radiofrequency ablation of solid renal tumors. AJR. 2003; 180:1509–13. [PubMed: 12760910]
80. Mayo-Smith WW, Dupuy DE, Parikh PM, et al. Imaging-guided percutaneous radiofrequency ablation of solid renal masses: technique and outcomes of 38 treatment sessions in 32 consecutive patients. AJR. 2003; 180:1503–8. [PubMed: 12760909]
81. Roy-Choudhury SH, Cast JE, Cooksey G, et al. Early experience with percutaneous radiofrequency ablation of small solid renal masses. AJR. 2003; 180:1055–61. [PubMed: 12646454]
82. Su LM, Jarrett TW, Chan DYS, et al. Percutaneous computed tomography-guided radiofrequency ablation of renal masses in high surgical risk patients: preliminary results. Urology. 2003; 61:26–33. [PubMed: 12657358]
83. Zagoria RJ, Hawkins AD, Clark PE, et al. Percutaneous CT-guided radiofrequency ablation of renal neoplasms: factors influencing success. AJR. 2004; 183:201–7. [PubMed: 15208139]
84. Gervais DA, McGovern FJ, Arellano RS, et al. Radiofrequency ablation of renal cell carcinoma: part 1, indications, results, and role in patient management over 6-year period and ablation of 100 tumors. AJR. 2005; 185:64–71. [PubMed: 15972400]
85. Varkarakis IM, Allaf ME, Inagaki T, et al. Percutaneous radiofrequency ablation of renal masses: results at a 2-year mean followup. J Urol. 2005; 174:456–60. [PubMed: 16006864]
86. Lewin JS, Connell CF, Duerk JL, et al. Interactive MRI-guided radiofrequency interstitial thermal ablation of abdominal tumors: clinical trial for evaluation of safety and feasibility. JMRI. 1998; 8:40–7. [PubMed: 9500259]
87. Lewin JS, Nour SG, Connell CF, et al. Phase II clinical trial of interactive MR imaging-guided interstitial radiofrequency thermal ablation of primary kidney tumors: initial experience. Radiology. 2004; 232(3):835–45. [PubMed: 15333798]
88. Merkle EM, Shonk JR, Duerk JL, et al. MR-guided RF thermal ablation of the kidney in a porcine model. AJR Am J Roentgenol. 1999; 173(3):645–51. [PubMed: 10470895]
89. Boss A, Clasen S, Kuczyk M, et al. Magnetic resonance-guided percutaneous radiofrequency ablation of renal cell carcinomas: a pilot clinical study. Invest Radiol. 2005; 40(9):583–90. [PubMed: 16118551]
90. Boss A, Clasen S, Kuczyk M, et al. Image-guided radiofrequency ablation of renal cell carcinoma. Eur Radiol. 2007; 17(3):725–33. [PubMed: 17021704]
91. Merkle EM, Nour SG, Lewin JS. MR imaging follow-up after percutaneous radiofrequency ablation of renal cell carcinoma: findings in 18 patients during first 6 months. Radiology. 2005; 235(3):1065–71. [PubMed: 15914485]
92. Memarsadeghi M, Schmook T, Remzi M, et al. Percutaneous radiofrequency ablation of renal tumors: midterm results in 16 patients. Eur J Radiol. 2006; 59(2):183–9. [PubMed: 16725292]
93. Kawamoto S, Permpongkosol S, Bluemke DA, et al. Sequential changes after radiofrequency ablation and cryoablation of renal neoplasms: role of CT and MR imaging. Radiographics. 2007; 27(2):343–55. [PubMed: 17374857]
94. Atwell TD, Farrell MA, Callstrom MR, et al. Percutaneous cryoablation of 40 solid renal tumors with US guidance and CT monitoring: initial experience. Radiology. 2007; 243:276–83. [PubMed: 17329689]
95. Atwell TD, Farrell MA, Callstrom MR, et al. Percutaneous cryoablation of large renal masses: technical feasibility and short-term outcome. AJR. 2007; 188:1195–200. [PubMed: 17449758]
96. Matina SF, Ahrarb K, Cadedduc JA, et al. Residual and recurrent disease following renal energy ablative therapy: a multi-institutional study. J Urol. 2006; 176:1973–7. [PubMed: 17070224]
97. Allaf ME, Varkarakis IM, Bhayani SB, et al. Pain control requirements for percutaneous ablation of renal tumors: cryoablation versus radiofrequency ablation—initial observations. Radiology. 2005; 237:366–70. [PubMed: 16126920]

98. Tacke J, Speetzen R, Heschel I, et al. Imaging of interstitial cryotherapy—an in vitro comparison of ultrasound, computed tomography, and magnetic resonance imaging. Cryobiology. 1999; 38:250–9. [PubMed: 10328915]
99. Saliken J, McKinnon J, Gray R. CT for monitoring cryotherapy. AJR. 1996; 166:853–5. [PubMed: 8610562]
100. Sandison GA, Loye MP, Rewcastle JC, et al. X-ray CT monitoring of iceball growth and thermal distribution during cryosurgery. Phys Med Biol. 1998; 43:3309–24. [PubMed: 9832018]
101. Gupta A, Allaf ME, Kavoussi LR, et al. Computerized tomography guided percutaneous renal cryoablation with the patient under conscious sedation: initial clinical experience. J Urol. 2006; 175:447–53. [PubMed: 16406968]
102. Permpongkosol S, Link RE, Kavoussi LR, et al. Percutaneous computerized tomography guided cryoablation for localized renal cell carcinoma: factors influencing success. J Urol. 2006; 176:1963–8. [PubMed: 17070219]
103. Littrup PJ, Ahmed A, Aoun HD, et al. CT-guided percutaneous cryotherapy of renal masses. J Vasc Interv Radiol. 2007; 18:383–92. [PubMed: 17377184]
104. Harada J, Dohi M, Mogami T, et al. Initial experience of percutaneous renal cryosurgery under the guidance of a horizontal open MRI system. Radiat Med. 2001; 19:291–6. [PubMed: 11837579]
105. Shingleton WB, Sewell J, Patrick E. Percutaneous renal tumor cryoablation with magnetic resonance imaging guidance. J Urol. 2001; 165:773–6. [PubMed: 11176465]
106. Shingleton WB, Sewell PE. Percutaneous renal cryoablation of renal tumors in patients with von Hippel-Lindau disease. J Urol. 2002; 167:1268–70. [PubMed: 11832711]
107. Shingleton WB, Sewell PE. Percutaneous cryoablation of renal cell carcinoma in a transplanted kidney. BJU International. 2002; 90:137–8. [PubMed: 12081786]
108. Sewell PE, Howard JC, Shingleton WB, et al. Interventional magnetic resonance image-guided percutaneous cryoablation of renal tumors. South Med J. 2003; 96:708–10. [PubMed: 12940328]
109. Shingleton WB, Sewell PE. Cryoablation of renal tumours in patients with solitary kidneys. BJU International. 2003; 92:237–9. [PubMed: 12887474]
110. Kodama Y, Abo D, Sakuhara Y, et al. MR-guided percutaneous cryoablation for bilateral multiple renal cell carcinoma. Radiat Med. 2005; 23:303–7. [PubMed: 16012408]
111. Silverman SG, Tuncali K, vanSonnenberg E, et al. Renal tumors: MR imaging guided percutaneous cryotherapy–initial experience in 23 patients. Radiology. 2005; 236:716–24. [PubMed: 16040927]
112. Miki K, Shimomura T, Yamada H, et al. Percutaneous cryoablation of renal cell carcinoma guided by horizontal open magnetic resonance imaging. Int J Urol. 2006; 13:880–4. [PubMed: 16882047]
113. Silverman SG, Tuncali K, Adams DF, et al. MR imaging-guided percutaneous cryotherapy of liver tumors: initial experience. Radiology. 2000; 217:657–64. [PubMed: 11110925]
114. Farrell MA, Charboneau JW, Callstrom MR, et al. Paranephric water instillation: a technique to prevent bowel injury during percutaneous renal radiofrequency ablation. AJR. 2003; 181:1315–7. [PubMed: 14573426]
115. Tuncali K, Morrison PR, Tatli S, et al. MRI-guided percutaneous cryoablation of renal tumors: use of external manual displacement of adjacent bowel loops. Eur J Radiol. 2006; 59:198–202. [PubMed: 16716551]
116. Elhawary H, Zivanovic A, Davies B, et al. A review of magnetic resonance imaging compatible manipulators in surgery. Proc Inst Mech Eng [H]. 2006; 220(3):413–24.

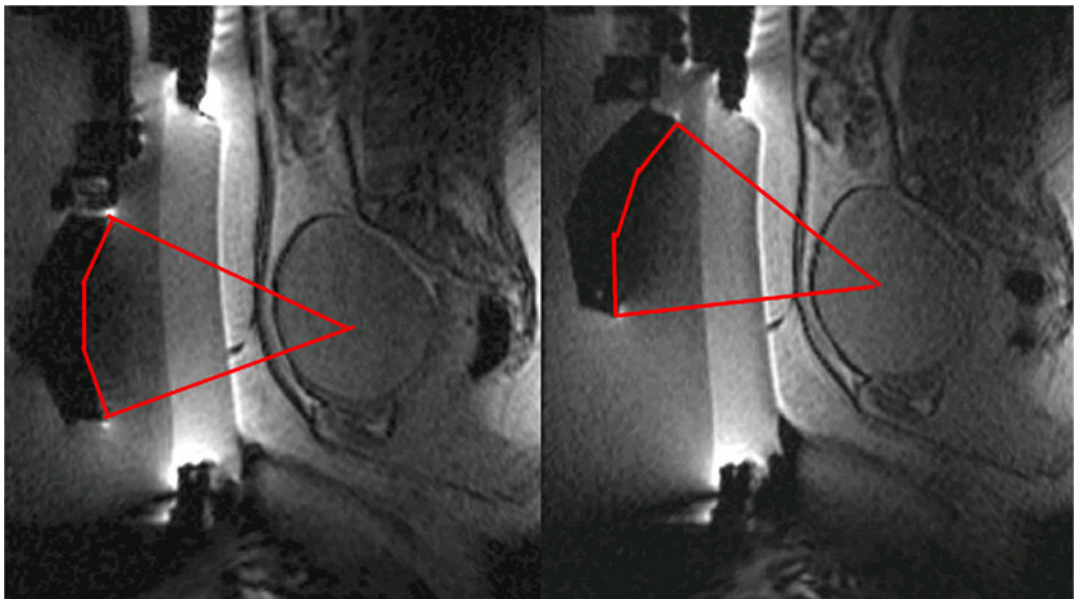

Fig. 1.

Linear scar through the subcutaneous tissue lies between the transducer and the fibroid, on the sagittal localizer image on the *left*. The sagittal localizer image on the *right* is obtained after tilting the transducer superiorly, without moving the patient, allowing treatment planning that will not course through the anterior abdominal subcutaneous tissue scar. (*Reproduced from* Fennessy FM, Tempany CM. A review of magnetic resonance imaging-guided focused ultrasound surgery of uterine fibroids. Top Magn Reson Imaging 2006;17(3):173–9; with permission.)

Fig. 2.

The sagittal localizer image on the *left* demonstrates bowel loops coursing between the anterior abdominal wall and the uterine fibroid. After placement of a spacer device (sagittal localizer image on the *right*) under the anterior abdominal wall, the bowel loops are displaced, allowing for treatment through a larger acoustic window. (*Reproduced from* Fennessy FM, Tempany CM. A review of magnetic resonance imaging-guided focused ultrasound surgery of uterine fibroids. Top Magn Reson Imaging 2006;17(3):173–9; with permission.)

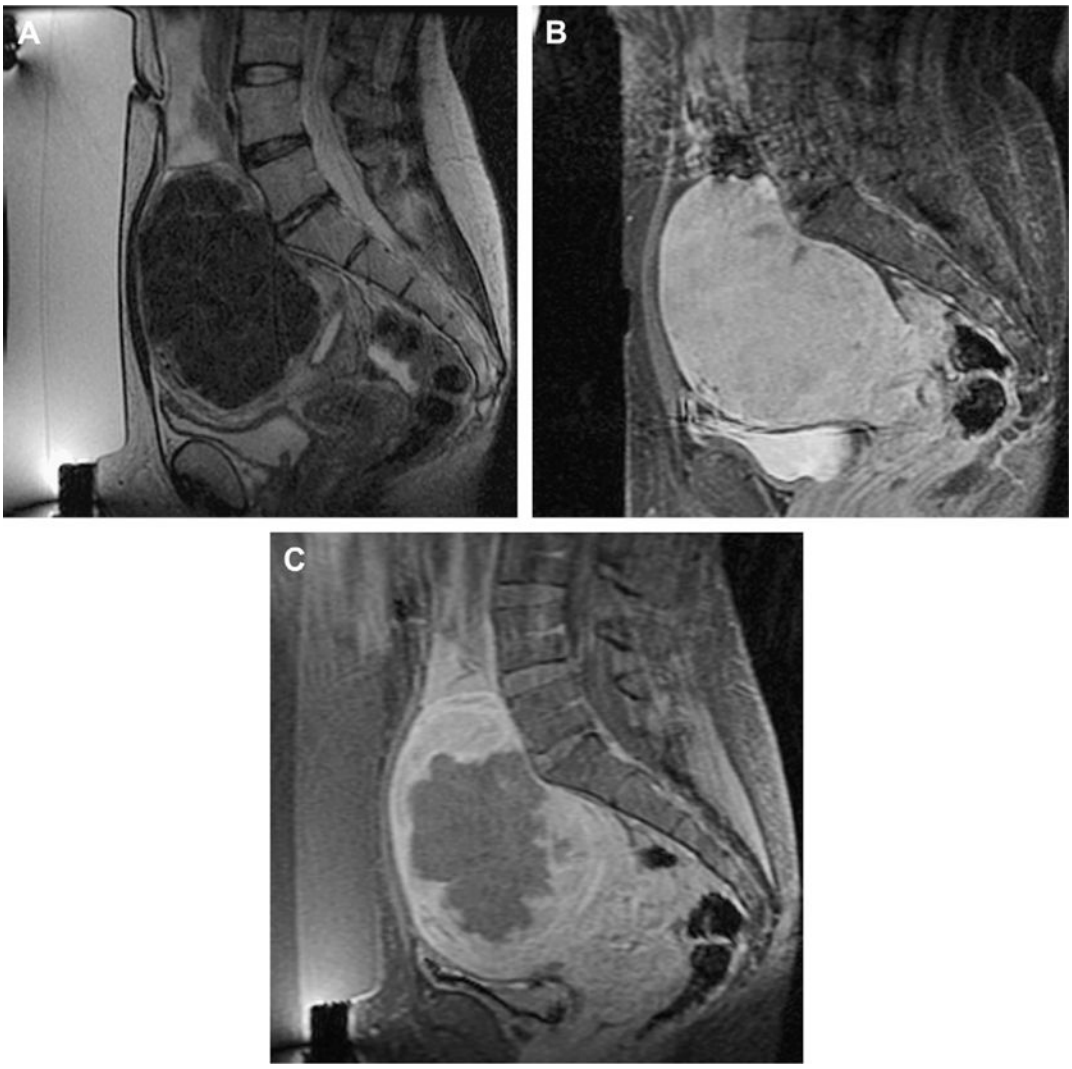

Fig. 3.

Imaging of a uterine fibroid pretreatment (*A*, *B*) and post-treatment (*C*) with MRgFUS. Sagittal T2-weighted image (*A*), obtained with the patient in the prone position overlying the US transducer, demonstrates a large solitary uterine fibroid of low-signal intensity. Sagittal SPGR post gadolinium (*B*) demonstrates homogenous enhancement of the fibroid. After treatment, sagittal SPGR post gadolinium (*C*) demonstrates a new large nonperfused area within the fibroid, consistent with treatment-induced necrosis.

Fig. 4.

Photograph demonstrating the set-up for percutaneous MR imaging–guided cryotherapy for uterine fibroids in an open horizontal 0.3-T AIRIS II (Hitachi, Tokyo, Japan) scanner. (*Courtesy* of Yusuke Sakuhara, MD, Department of Radiology, Hokkaido University Hospital, Sapporo, Japan.)

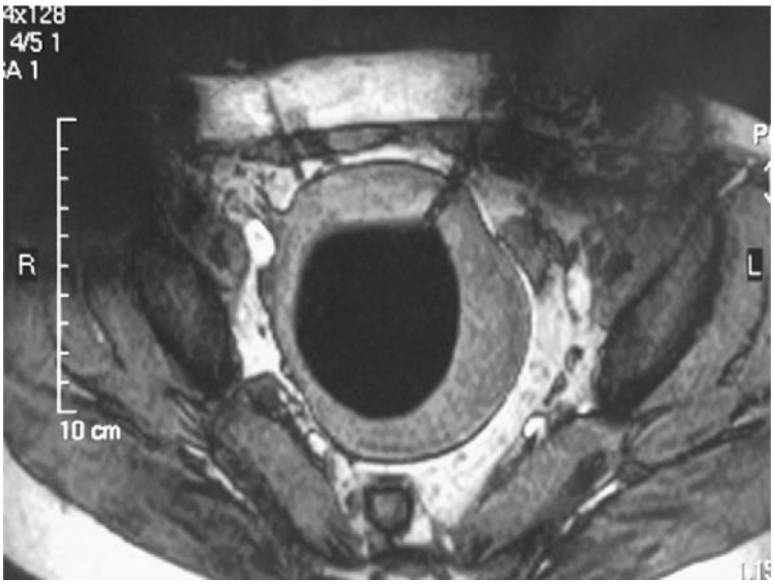

Fig. 5.

Axial T2-weighted spin-echo sequence demonstrating a probe in the left anterolateral aspect of a uterine fibroid. The diffuse low-signal intensity in the fibroid represents the ice-ball. (*Courtesy* of Yusuke Sakuhara, MD, Department of Radiology, Hokkaido University Hospital, Sapporo, Japan.)

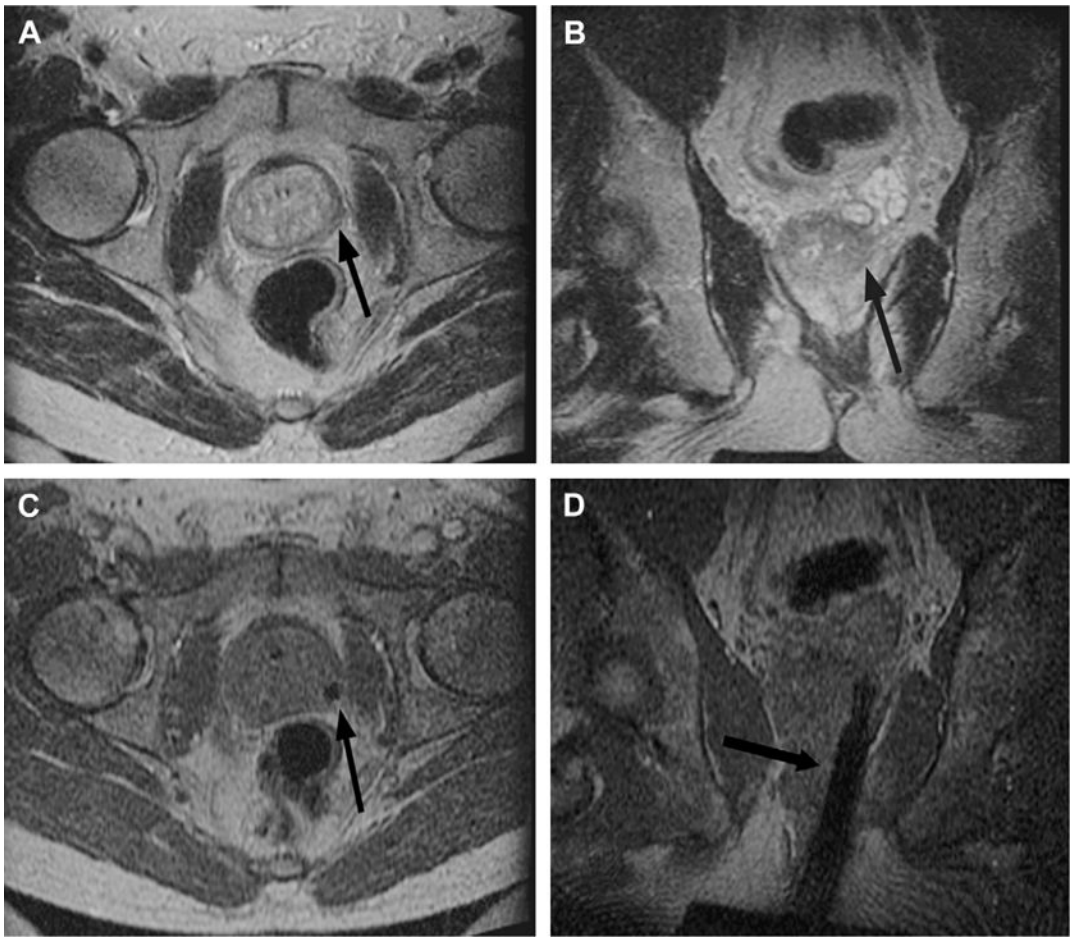

Fig. 6.

Imaging before and during MR imaging–guided prostate biopsy. Axial (*A*) and coronal (*B*) T2-weighted spin-echo sequence outline areas to be biopsied. In this example, an area in the left midgland is demonstrated (*arrow*), reformatted to the same spatial location as the corresponding real-time axial (*C*) and coronal images (*D*) taken during needle insertion. The biopsy needle is seen in cross section as a circle of low-signal intensity (*arrow*) on the axial gradient-echo real-time image (*C*) and as a longitudinal area of low-signal intensity (*arrow*) on the coronal gradient-echo real-time image (*D*).

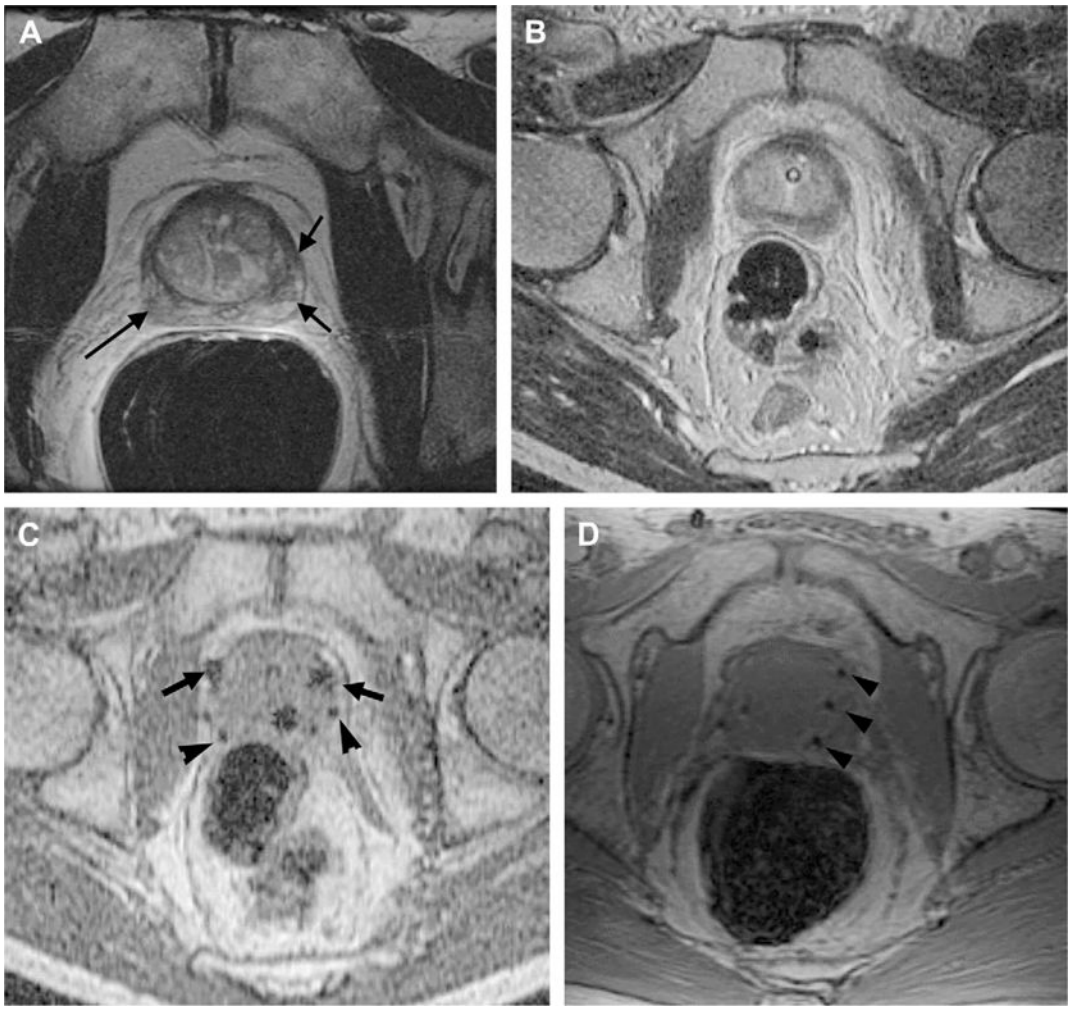

Fig. 7.

Pre-, intra-, and postoperative MR imaging–guided brachytherapy in prostate cancer. Preoperative 1.5-T (*A*) axial T2-weighted spin-echo image through the prostate base, demonstrating low signal intensity in the peripheral zone (*arrows*), previously demonstrated to be tumor. Intraoperative 0.5-T (*B*) axial T2-weighted spin-echo T2 weighted spin-echo image through the same area. Intraoperative axial gradient-echo MR images (*C*) obtained in real time during needle and seed placement in the prostate base. The larger round areas represent the needles (*arrows*), before deployment, and the small round areas represent the deployed seeds (*arrowheads*). A postoperative axial SPGR (*D*) through the prostate base demonstrates multiple round areas of low signal in the peripheral zone (*arrowheads*), consistent with deployed seeds.

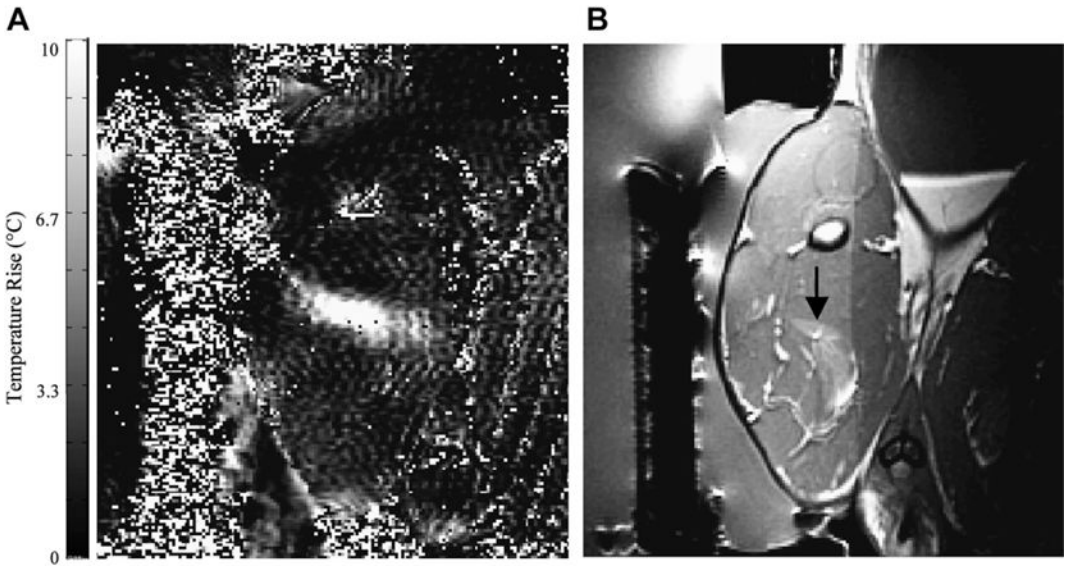

Fig. 8.

(*A*) MR imaging–based temperature image during a sonication (130 W for 30 seconds) into rabbit thigh muscle during a test of an MR imaging–compatible transrectal phased array applicator for MRgFUS of prostate. (*B*) The thermal lesion (*arrow*) seen in T2-weighted imaging. The bright region to the right of the lesion is a tissue fascia layer. (*From* Sokka SD, Hynynen K. The feasibility of MRI-guided whole prostate ablation with a linear aperiodic intracavitary ultrasound phased array. Phys Med Biol 2000;45:3373–83; with permission.)

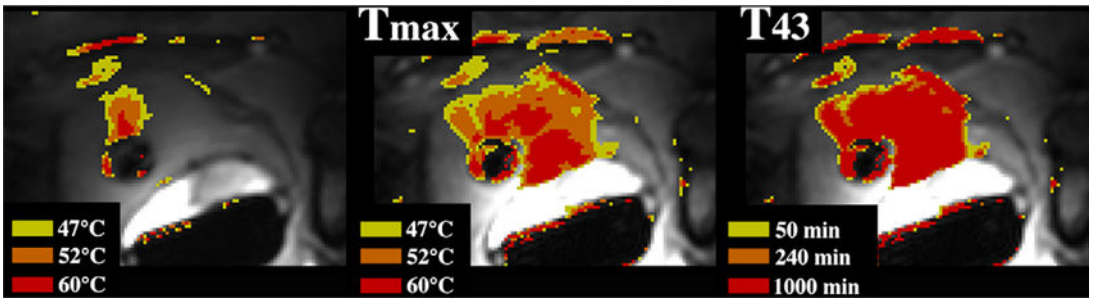

Fig. 9.

MR imaging–guided catheter-based US thermal therapy of the prostate: real-time temperature image (*left*), maximum temperature image (*middle*), and thermal dose (*right*) of the prostate during catheter-based US thermal therapy. The transurethral catheter, with a rotating curvilinear transducer array, is depicted as the round low-signal intensity structure within the prostate gland.[69] (*Courtesy* of Kim Butts Pauly, PhD, Viola Rieke, MD, and Graham Sommer,PhD, Stanford University School of Medicine, Stanford, CA; and Chris Diederich, PhD, UCSF, SanFrancisco, CA.)

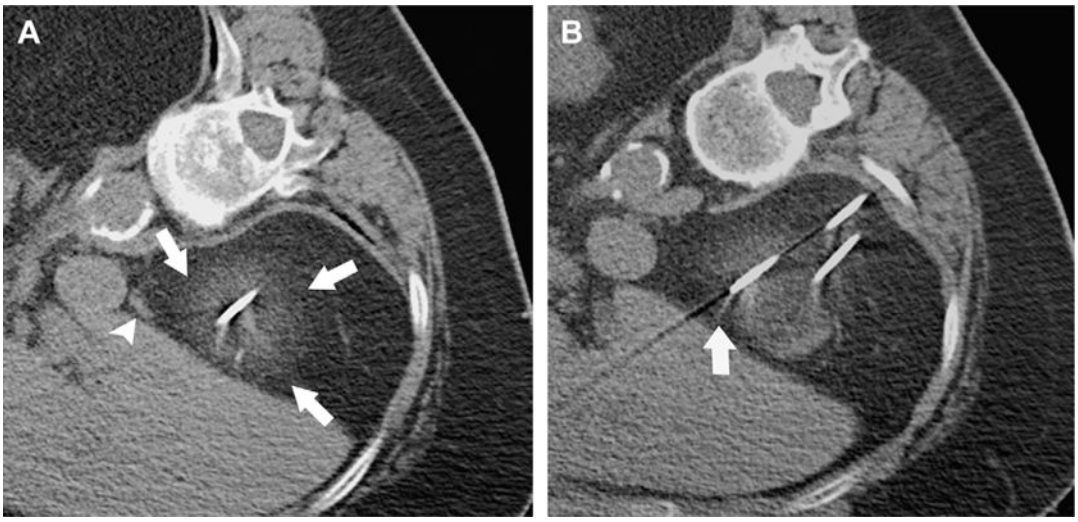

Fig. 10.

CT–guided percutaneous cryotherapy of renal yumors. A 77-year-old woman who had RCC of the right kidney upper pole. Unenhanced transverse CT images obtained during percutaneous cryoablation performed in the right lateral decubitus position show that (*A*) low contrast-to-noise ratio and poor edge definition of ice ball (*arrows*) in the perinephric fat renders assessment for overlap of ablation zone with adjacent adrenal gland (*arrowhead*) difficult, and (*B*) streak artifact from applicator interferes with visualization of portion of the ice ball (*arrow*).

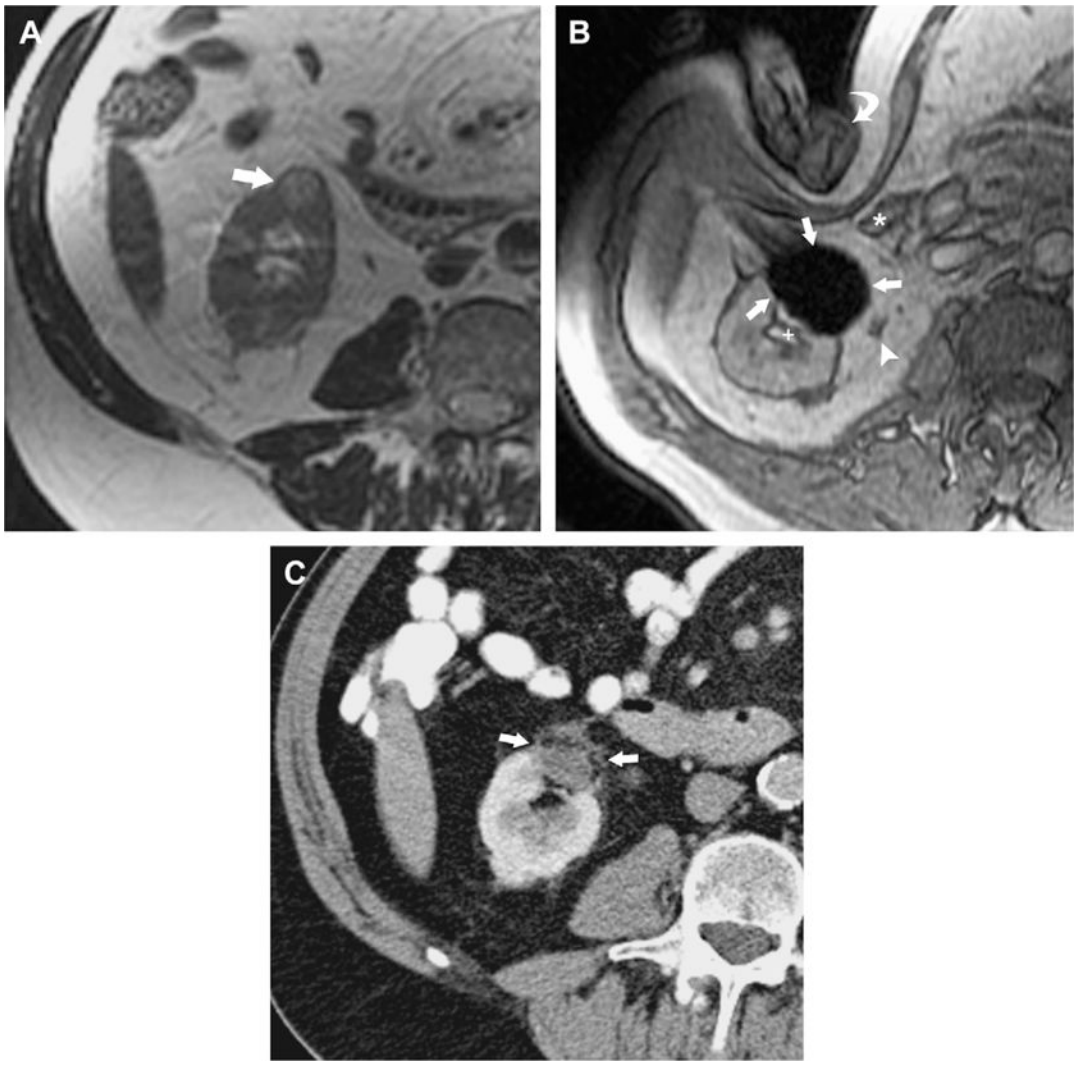

Fig. 11.

MR imaging–guided percutaneous cryotherapy of renal tumor. A 70-year-old man who had RCC of the right kidney lower pole treated with MR imaging–guided percutaneous cryoablation. (*A*) Transverse T2-weighted fast recovery fast spin–echo sequence image obtained before treatment in 1.5-T MR image shows a small exophytic renal mass in the lower pole of the right kidney anteriorly (*arrow*). (*B*) Intraprocedural transverse gradient-echo image obtained in 0.5-T open configuration interventional MR imaging shows that sharp edge definition of signal void ice ball (*arrows*) contributes to monitoring of tumor coverage and assessment of proximity to adjacent ureter (*arrowhead*), renal collecting system (+), and colon (*), which is being displaced by an interventionalist's hand (*curved arrow*). (*C*) An 18-month follow-up contrast-enhanced transverse CT image shows no enhancement in the involuted ablation zone (*arrows*).